International Journal of Engineering

Journal Homepage: www.ije.ir

Mixed-mode Multiphase Sinusoidal Oscillators using Differential Voltage Current Conveyor Transconductance Amplifiers and Only Grounded Passives Components

T. Phianpranthong[a], A. Suksawad[b], A. Jantakun*[a]

[a] *Electronics and Telecommunication Engineering Department, Faculty of Engineering, Rajamangala University of Technology Isan, Khon Kaen Campus, Khon Kaen, Thailand*
[b] *Computer Engineering Department, Faculty of Engineering, Rajamangala University of Technology Isan, Khon Kaen Campus, Khon Kaen, Thailand*

PAPER INFO

Paper history:
Received 31 October 2022
Received in revised form 10 December 2022
Accepted 10 December 2022

Keywords:
Mixed-mode
Multiphase Sinusoidal Oscillators
Grounded Passive Component
Gain-controllable
Low-pass Filter
High Impedance

ABSTRACT

This article is about mixed-mode multiphase sinusoidal oscillators that are made up of differential voltage current conveyor transconductance amplifier (DVCCTA) and use all the grounded passive components. The proposed multiphase sinusoidal oscillators provide a single DVCCTA, a single grounded resistor and a capacitor for each phase which is suitable for integrated circuit implementation. In addition, the sinusoidal outputs generate currents and voltages simultaneously. The current signals from the outputs have high impedances, which make it easier to connect them directly to the next circuit or stage. The proposed circuits can generate multiphase sinusoidal signals that are both equally phased and in amplitude. The oscillation can be adjusted simultaneously of the frequency of oscillation by the electronic method. A simulation with the PSPICE program and an experiment with commercially available ICs (AD830, AD844, and LM13700N) demonstrated. The results show the efficiency of the circuit is completely consistent with the theory.

***doi**: 10.5829/ije.2023.36.05b.18*

1. INTRODUCTION

The multiphase sinusoidal oscillator (MSO) has come to be part of electrical and electronic engineering; which makes it an important component. MSO is widely used in many fields, such as communications, where it is used in phase modulators, quadrature mixers, and single-sideband generators [1, 2], in power electronics systems for work related to a three-phase induction motor drive [3], and in measurement systems, where it is used for the selective voltmeters and vector generators [4]. From research and reviews of the literature, many researchers and publishers have suggested different ways to design the MSO, such as by using a low-pass filter, high-pass filter, and all-pass filter, which used active building 1blocks at high performance in development [5-24]. Table 1 summarized the various MSOs have different advantages: a single active building block is used per phase of [7-11, 13-24], which makes it easy to assemble for simulation and experimentation, the passive elements that have been used in minimal numbers in the literture [5-12, 14, 16, 19-24]. MSOs are all grounded, where a grounded capacitor is attractive for integrated circuit implementation. The design techniques of MSOs in literture [5, 6, 9, 10, 13, 15, 17-24] do not require additional amplifier circuit for sinusoidal oscillation. The condition of oscillation (CO) can easily be adjusted electronically by a microcontroller or microcomputer [25, 26]. In addition, some research has shown the results of experiments with commercially available integrated circuits (ICs) [5, 7-9, 15, 18]. However, in various MSOs, it was also found that there were various weaknesses as follow. Jaikla et al. [5], Thongdit et al. [6] and Tangsrirat et al. [12] reported that more than one active building block is used per phase. Skotis and Psychalinos [8], Wu et al. [9] Jaikla et al. [13], Klahan et al. [15], Pandey et

*Corresponding Author Institutional Email: Adirek.ja@rmuti.ac.th
(A. Jantakun)

Please cite this article as: T. Phianpranthong, A. Suksawad, A. Jantakun, Mixed-mode Multiphase Sinusoidal Oscillators using Differential Voltage Current Conveyor Transconductance Amplifiers and Only Grounded Passives Components, ***International Journal of Engineering, Transactions B: Applications***, Vol. 36, No. 05, (2023) 1023-1033

TABLE 1. Comparison between various MSOs

Ref.	(a)	(b)	(c)	(d)	(e)	(f)	(g)	(h)	(i)	(j)
Jaikla et al. [5]	OTA	2	High-pass filter	Yes	1+1	No	Yes	Voltage	-	Yes
Thongdit et al. [6]	OTA	2	High-pass filter	Yes	0+1	No	Yes	Current	Yes	No
Prommee and Dejhan [7]	OTA	1	Low-pass filter	Yes	0+1	Yes	Yes	Voltage	-	Yes
Skotis and Psychalinos [8]	CCII	1	Low-pass filter	Yes	2+1	Yes	No	Voltage	-	Yes
Wu et al. [9]	CCII	1	Low-pass filter	Yes	2+1	No	No	Voltage	-	Yes
Abuelma'atti and Al-Qahtani [10]	CCCII	1	Low-pass filter	Yes	0+2	No	Yes	Current	Yes	No
Loescharataramdee et al. [11]	CCCII	1	Low-pass filter	Yes	0+1	Yes	Yes	Current	Yes	No
Tangsrirat et al. [12]	CDTA	2	All-pass filter	No	0+1	Yes	Yes	Current	Yes	No
Jaikla et al. [13]	CDTA	1	All-pass filter	No	2+1	No	Yes	Current	Yes	No
Tangsrirat and Tanjaroen [14]	CDTA	1	Low-pass filter	Yes	0+1	Yes	Yes	Current	Yes	No
Klahan et al. [15]	CDBA	1	Low-pass filter	No	2+1	No	No	Voltage	-	Yes
Sagbas et al. [16]	CBTA	1	Low-pass filter	Yes	0+1	Yes	Yes	Voltage	-	No
Pandey et al. [17]	OTRA	1	All-pass filter	No	3+1	No	No	Voltage	-	No
Pandey and Bothra [18]	OTRA	1	Low-pass filter	No	2+1	No	No	Voltage	-	Yes
Jaikla and Prommee [19]	CCCDTA	1	All-pass filter	Yes	1+1	No	Yes	Current	Yes	No
Kumngern [20]	CCCDTA	1	Low-pass filter	Yes	0+1	No	Yes	Current	Yes	No
Kumngern [21]	CCCDTA	1	High-pass filter	Yes	0+1	No	Yes	Current	Yes	No
Uttaphut et al. [22]	CCCCTA	1	All-pass filter	Yes	0+1	No	Yes	Current	Yes	No
Gupta and Pandey [23]	DO-VDBA	1	All-pass filter	No	0+1	No	Yes	Voltage	-	No
Pitaksuttayaprot et al. [٢٤]	VDCC	١	Low-pass filter	Yes	٢+١	No	Yes	Current	Yes	Yes
This work MSOs	DVCCTA	1	Low-pass filter	Yes	1+1	No	Yes	Current/Voltage	Yes	Yes

Remarks: (a) Active element (b) No. of active element per phase (c) Design technique (d) All grounded passive elements
(e) No. of R+C per phase (f) Additional amplifier (g) Electronic tune CO (h) Output type
(i) High output impedance for current-mode (j) Experimental results

al. [17], Pandey and Bothra [18] reported a large number of resistors and capacitors are used, making the area of the integrated circuit (IC) larger. A floating capacitor has been used in literature [12-13, 17-18, 23], which are unsuitable for fabrication in an integrated circuit. The circuits reported in litertaure [7-8, 11-12, 14, 16] required additional amplifiers for sinusoidal oscillation. The stated conditions of oscillation in litertaure [8-9, 15, 17-18] cannot be adjusted electronically.

The aim of this paper is to propose the use of three MSOs using a single differential voltage current conveyor transconductance amplifier (DVCCTA), a single resistor, and a single capacitor per phase, and to make use of all the grounded passive components. The current outputs have a high impedance and are directly connected to loads. The proposed circuits provide multiphase signals that are equally spaced in phase and of equal amplitude. It does not need additional amplifiers for oscillation as it can be adjusted electronically. In addition, the proposed MSOs show that the simulation results with the PSPICE program and experimental results with commercially available ICs agree well with the theoretical analysis.

2. PRINCIPLE OF OPERATION

This topic presents the electrical characteristics of the differential voltage current conveyor transconductance amplifier as an active building block. It was used as the basis for the design of the proposed MSOs. Next is analysis of the various working operations of MSOs, and last is a non-ideal case analysis of the proposed circuits.

2. 1. Differential Voltage Current Conveyer Transconductance Amplifier The differential voltage current conveyor transconductance amplifier (DVCCTA) was used in the synthesis of the proposed MSOs. The DVCCTA was published by Jantakun et al. [27]. It shows the details of the electrical symbols and equivalent circuits in Figure 1, which has various terminals as follow: terminals (Y_1 and Y_2) are input

voltages, the voltage (V_X) at the X terminal is the difference between the input voltages V_{Y1} and V_{Y2}, the current (I_Z) at the Z terminal is obtained by mirroring the current (I_X) which is of equal amplitude, the output current (I_O) at the O terminal is caused by multiplying the transconductance (g_m) and the voltage (V_Z). In addition, these terminals have high impedance except for the X terminal. The characteristics equation of DVCCTA can be written by the relative voltage and current as follows:

$$\begin{pmatrix} I_{Y1} \\ I_{Y2} \\ V_X \\ I_Z \\ I_O \end{pmatrix} = \begin{pmatrix} 0 & 0 & 0 & 0 & 0 \\ 0 & 0 & 0 & 0 & 0 \\ 0 & 1 & -1 & 0 & 0 \\ 1 & 0 & 0 & 0 & 0 \\ 0 & 0 & 0 & \pm g_m & 0 \end{pmatrix} \begin{pmatrix} I_X \\ V_{Y1} \\ V_{Y2} \\ V_Z \\ V_O \end{pmatrix}. \quad (1)$$

The DVCCTA of the proposed circuit is implemented by BJT technology. The transconductance (g_m) can be written as follows:

$$g_m = \frac{I_B}{2V_T}. \quad (2)$$

From Equation (2), the transconductance (g_m) can be adjusted electronically with the DC bias current (I_B). The thermal voltage (V_T) is equal to 26 mV at room temperature.

2. 2. DVCCTA-based Gain-controllable Low-pass Filter The gain-controllable lossy integrator, which is also known as the gain-controllable low-pass filter is shown here since the proposed MSOs are based-on these integrators. The DVCCTA-based gain controlled low-pass filters are shown in Figure 2. The current transfer function of Figures 2(a), 2(b), and 2(c) can be found in Table 2, which can be derived from the DVCCTA features. The current output can be constructed to work with non-inverting or inverting signals, as the current transfer function can act as either non-inverting or inverting gain-controllable low-pass filter.

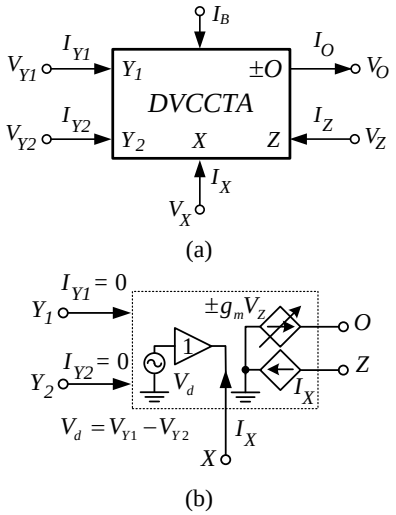

Figure 1. DVCCTA (a) electrical symbol (b) equivalent circuit

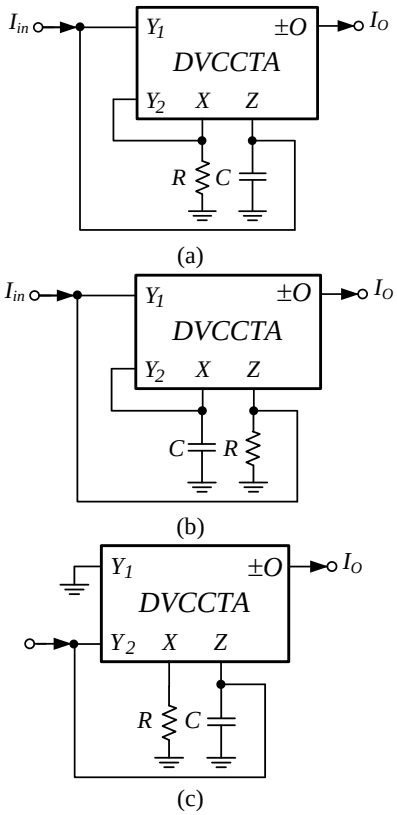

Figure 2. Gain-controllable low-pass filter

TABLE 2. The current transfer function of Figure 2

Figure	Transfer function
2 (a)	$\frac{I_O(s)}{I_{in}(s)} = \pm\frac{2g_mR}{2sRC+1}$
2 (b)	$\frac{I_O(s)}{I_{in}(s)} = \pm\frac{g_mR}{sRC/2+1}$
2 (c)	$\frac{I_O(s)}{I_{in}(s)} = \pm\frac{g_mR}{sRC+1}$

It is clear that all three circuits of the gain-controllable low-pass filters have the same capability. This capability is that the circuit consists of one DVCCTA, one grounded resistor, and one grounded capacitor. Additionally, the circuit can be electronically tuned by adjusting the transconductance gain g_m of the DVCCTA, making it appropriate for IC implementation [28-30]. Furthermore, it has high output impedances, allowing for simple cascading in current-mode configurations.

2. 3. The Proposed Mixed-mode Multiphase Sinusoidal Oscillator The proposed three mixed-mode multiphase sinusoidal oscillators, which are odd-phase MSO, in Figures 3(a), 3(b), and 3(c) are implemented. They are cascading the N identical stages (N ≥ 3, 5, 7….) of the DVCCTA-based inverting gain-controllable low-pass filters for each phase. The sinusoidal signals are simultaneously generated for both the current and the voltage-mode. The sinusoidal current outputs are high impedance that can be cascaded directly to load or the next stage without any additional current amplifiers. However, the voltage outputs must be used with voltage buffers to make it connect to the next stage. Also, the even-phase MSO can be constructed by cascading non-inverting and inverting gain-controllable low-pass filters, as explained and reported in literature [31]. The transconductance and passive components in MSOs satisfy the equality conditions g_m, C, and R. The parameters of MSOs can be then analyzed, and the results are summarized in Table 3. They provide the loop gain of the system, the characteristic equation, the CO and FO, and the phase relationship. When the CO and FO are set up, the steady-state magnitude ratios of the sinusoidal signals for voltages and currents show the same magnitude, as presented in Table 4. The output amplitude level of each gain-controllable low-pass filter may be easily stabilized using an optocoupler and photoresistor that is described in literature [32].

It is clearly seen that the three mixed-mode MSOs have the same ability, which is the CO can be tuned electronically/simultaneously of the FO by adjusting the DC bias current of DVCCTAs. Furthermore, when the CO and FO are archived, the ratio of output signals are close to unity. Consequently, the output signals are equally in amplitude and spaced in phase with respect to all oscillation frequencies.

2. 4. Non-ideal Case Analysis of The Proposed Circuits The non-ideal analysis of the proposed circuits is important to take the non-idealities of

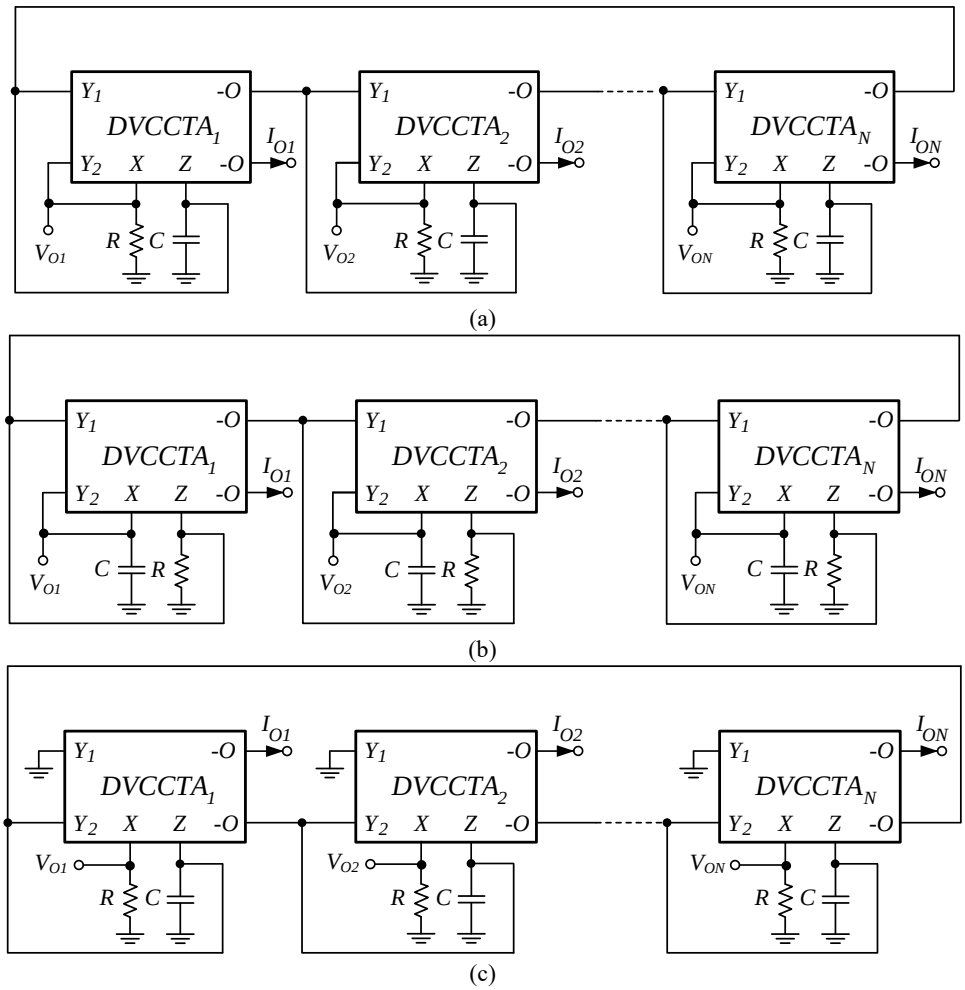

Figure 3. The proposed MSOs

TABLE 3. The MSOs parameters

Figure	(a)	(b)	(c)	(d)	(e)
3 (a)	$\left[\frac{-2g_mR}{2RCs+1}\right]^N=1$	$\left(j\omega_{osc}2RC+1\right)^N+(-1)^{N+1}\left(2g_mR\right)^N=0$	$2g_mR\geq\sqrt{1+\tan^2\frac{\pi}{N}}$	$\omega_{osc}=\frac{1}{2RC}\tan\frac{\pi}{N}$	$\phi=\frac{2\pi}{N}$
3 (b)	$\left[\frac{-g_mR}{s\frac{RC}{2}+1}\right]^N=1$	$\left(j\omega_{osc}\frac{RC}{2}+1\right)^N+(-1)^{N+1}\left(g_mR\right)^N=0$	$g_mR\geq\sqrt{1+\tan^2\frac{\pi}{N}}$	$\omega_{osc}=\frac{2}{RC}\tan\frac{\pi}{N}$	$\phi=\frac{2\pi}{N}$
3 (c)	$\left[\frac{-g_mR}{sRC+1}\right]^N=1$	$\left(j\omega_{osc}RC+1\right)^N+(-1)^{N+1}\left(g_mR\right)^N=0$	$g_mR\geq\sqrt{1+\tan^2\frac{\pi}{N}}$	$\omega_{osc}=\frac{1}{RC}\tan\frac{\pi}{N}$	$\phi=\frac{2\pi}{N}$

Remarks: (a) The system loop gain (LG) of the MSO circuits. (b) The frequency of oscillation $\omega_{osc}=2\pi f_{osc}$, the Barkhausen's condition. (c) The condition of oscillation (CO) .(d) The frequency of oscillation (FO) for *N*=3, 5, 7, …(e) The phase relations of output sinusoidal signals.

TABLE 4. The ratio between the output sinusoidal signals

Figure	The ratio of outputs
3 (a)	$\left\|\frac{I_{O2}(j\omega_{osc})}{I_{O1}(j\omega_{osc})}\right\|=\left\|\frac{I_{ON}(j\omega_{osc})}{I_{O2}(j\omega_{osc})}\right\|=\left\|\frac{I_{O1}(j\omega_{osc})}{I_{ON}(j\omega_{osc})}\right\|=\left\|\frac{V_{O2}(j\omega_{osc})}{V_{O1}(j\omega_{osc})}\right\|=\left\|\frac{V_{ON}(j\omega_{osc})}{V_{O2}(j\omega_{osc})}\right\|=\left\|\frac{V_{O1}(j\omega_{osc})}{V_{ON}(j\omega_{osc})}\right\|=\left\|\frac{2g_mR}{2RC\omega_{osc}+1}\right\|=1$
3 (b)	$\left\|\frac{I_{O2}(j\omega_{osc})}{I_{O1}(j\omega_{osc})}\right\|=\left\|\frac{I_{ON}(j\omega_{osc})}{I_{O2}(j\omega_{osc})}\right\|=\left\|\frac{I_{O1}(j\omega_{osc})}{I_{ON}(j\omega_{osc})}\right\|=\left\|\frac{V_{O2}(j\omega_{osc})}{V_{O1}(j\omega_{osc})}\right\|=\left\|\frac{V_{ON}(j\omega_{osc})}{V_{O2}(j\omega_{osc})}\right\|=\left\|\frac{V_{O1}(j\omega_{osc})}{V_{ON}(j\omega_{osc})}\right\|=\left\|\frac{g_mR}{\frac{RC\omega_{osc}}{2}+1}\right\|=1$
3 (c)	$\left\|\frac{I_{O2}(j\omega_{osc})}{I_{O1}(j\omega_{osc})}\right\|=\left\|\frac{I_{ON}(j\omega_{osc})}{I_{O2}(j\omega_{osc})}\right\|=\left\|\frac{I_{O1}(j\omega_{osc})}{I_{ON}(j\omega_{osc})}\right\|=\left\|\frac{V_{O2}(j\omega_{osc})}{V_{O1}(j\omega_{osc})}\right\|=\left\|\frac{V_{ON}(j\omega_{osc})}{V_{O2}(j\omega_{osc})}\right\|=\left\|\frac{V_{O1}(j\omega_{osc})}{V_{ON}(j\omega_{osc})}\right\|=\left\|\frac{g_mR}{RC\omega_{osc}+1}\right\|=1$

DVCCTA, which consist of the voltage and current tracking errors and the effects of the parasitic conponents, with details as follows:

2. 4. 1. The Voltage and Current Tracking Errors The voltage and current tracking errors of DVCCTA must be occurred by the mismatch of internal BJT which can be written with the characteristics equation as follows:

$$\begin{pmatrix} I_{Y1} \\ I_{Y2} \\ V_X \\ I_Z \\ I_O \end{pmatrix} = \begin{pmatrix} 0 & 0 & 0 & 0 & 0 \\ 0 & 0 & 0 & 0 & 0 \\ 0 & \gamma_1 & -\gamma_2 & 0 & 0 \\ \alpha & 0 & 0 & 0 & 0 \\ 0 & 0 & 0 & \pm\beta g_m & 0 \end{pmatrix} \begin{pmatrix} I_X \\ V_{Y1} \\ V_{Y2} \\ V_Z \\ V_O \end{pmatrix} \quad (3)$$

where the voltage tracking errors from Y_1 and Y_2 terminals to the *X* terminal are the γ_1 and γ_2. The current tracking error from *X* terminal to *Z* terminal is the α, and the voltage tracking error from *Z* terminal for transfer to *O* terminal is the β. The ideally values of α, β, and γ parameters are equal to unity. However, the influence of the voltage and current tracking errors can be examined for the proposed MSOs, as stated in Table 5.

2. 4. 2. The Effects of Parasitic Conponents The parasitic resistances and capacitances of DVCCTA are presented in Figure 4. The parasitic elements are connected to the ground at terminals Y_1, Y_2, Z, and O due to the presence of high impedances composed by parasitic resistances (R_{Y1}, R_{Y2}, R_Z, and R_O) and parasitic

TABLE 5. The CO and FO of MSOs by tracking errors effected

Figure	CO	FO
3 (a)	$2\gamma_2\beta gmR\geq\sqrt{1+\tan^2\frac{\pi}{N}}$	$\omega_{osc}=\frac{\gamma_2}{2\gamma_1RC}\tan\frac{\pi}{N}$
3 (b)	$\gamma_2\beta gmR\geq\sqrt{1+\tan^2\frac{\pi}{N}}$	$\omega_{osc}=\frac{2\gamma_2}{\gamma_1RC}\tan\frac{\pi}{N}$
3 (c)	$\beta g_mR\geq\sqrt{1+\tan^2\frac{\pi}{N}}$	$\omega_{osc}=\frac{\gamma_2}{RC}\tan\frac{\pi}{N}$

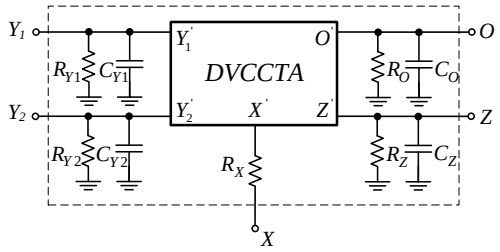

Figure 4. Non-ideal DVCCTA model

capacitances (C_{Y1}, C_{Y2}, C_Z, and C_O). Simultaneously, the X terminal has low impedance and has parasitic resistance (R_X) connected in series. In Table 6, the effects of parasitic resistances and capacitances on the performance of the proposed MSOs are evaluated and explained in detail. It can be observed that both the CO and FO have been influenced by parasitic elements. It is clear that these parasitic elements have downgraded the performance of the proposed MSOs.

TABLE 6. The CO and FO of MSOs by the parasitic elements effected

Figure	CO	FO	Settings of parasitic elements
3 (a)	$2g_m / Y_{T2}$ ³ $\sqrt{1+\tan^2\frac{\pi}{N}}$	$\omega_{osc} = \frac{1}{2Y_{T1}/Y_{T2}}\tan\frac{\pi}{N}$	$G_Z = \frac{1}{R_Z}, G_R = \frac{1}{R}, G_{Y1} = \frac{1}{R_{Y1}}, G_{Y2} = \frac{1}{R_{Y2}},$ $G_{T1} = G_Z + G_{Y1}, G_{T2} = G_R + G_{Y2}, sC_T = s(C_Z + C_{Y1} + C),$ $Y_{T1} = G_{T1} + sC_T, Y_{T2} = G_{T2} + sC_{Y2}$
3 (b)	g_m / Y_{T1} ³ $\sqrt{1+\tan^2\frac{\pi}{N}}$	$\omega_{osc} = \frac{2Y_{T1}}{Y_{T2}}\tan\frac{\pi}{N}$	$G_Z = \frac{1}{R_Z}, G_R = \frac{1}{R}, G_{Y1} = \frac{1}{R_{Y1}}, G_{Y2} = \frac{1}{R_{Y2}},$ $G_{T1} = G_Z + G_{Y1} + G_R, sC_{T1} = s(C_Z + C_{Y1}), sC_{T2} = s(C + C_{Y2}),$ $Y_{T1} = G_{T1} + sC_{T1}, Y_{T2} = G_{Y2} + sC_{T2}$
3 (c)	g_m / G_R ³ $\sqrt{1+\tan^2\frac{\pi}{N}}$	$\omega_{osc} = \frac{1}{Y_{T1}/G_R}\tan\frac{\pi}{N}$	$G_Z = \frac{1}{R_Z}, G_R = \frac{1}{R}, G_{Y2} = \frac{1}{R_{Y2}},$ $G_{T1} = G_Z + G_{Y2}, sC_T = s(C_Z + C_{Y2} + C),$ $Y_{T1} = G_{T1} + sC_T$

3. RESULTS OF SIMULATION AND EXPERIMENTAL

To prove the validity of the theoretical analysis, the proposed mixed-mode MSO circuit in Figure 3(c) was chosen as a simulation example. For example, $N = 3$ or three phase sinusoidal oscillators have been simulated through the PSPICE program. Figure 5 shows the internal construction of DVCCTA which is created by the PNP and NPN transistors using the parameters of the PR200N and NR200N bipolar transistors of the ALA400 transistor array from AT &T [32]. The setting of the condition of oscillation must have a value about of 2. In this arrangement, the resistors in the circuit have a standard value of $R = 2$ kΩ and DC bias current of $I_A = 50$ μA and $I_B = 50$ μA has been specified. The capacitor chooses a standard value of $C = 1$ nF and the power supply voltage

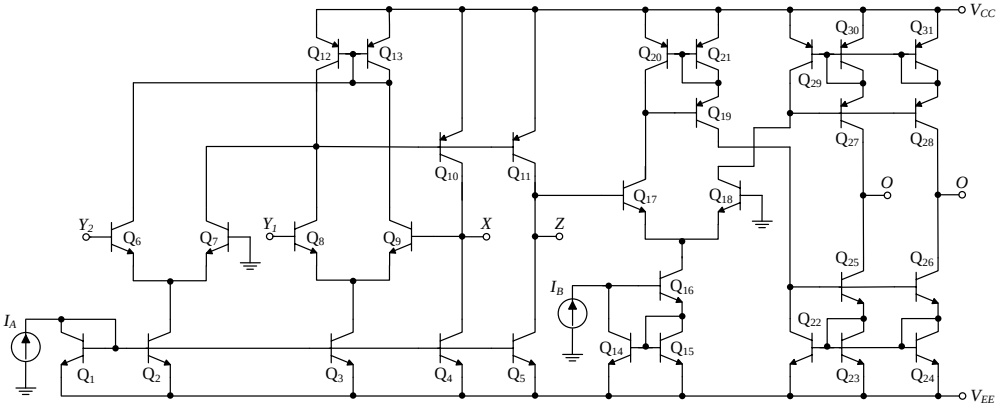

Figure 5. The internal construction of DVCCTA

is set at ±1.5 V. The proposed MSO waveforms of I_{O1}, I_{O2}, and I_{O3} have been simulated and plotted with two states, including: the transient-state at 0 to 1000 µs of time simulation, as shown in Figure 6, and the steady-state, as shown in Figure 7. The frequency spectrums of the sinusoidal signals which have a frequency of 137 kHz are presented in Figure 8. When compared to the theoretically determined frequency of 137.83 kHz, the sinusoidal signals have a frequency error of 0.60 % which may have been caused by a voltage and current tracking error, as well as by the parasitic components described in the previous section. The total harmonic distortions (THD) of sinusoidal signals I_{O1}, I_{O2}, and I_{O3} have values of 0.793%, 0.726%, and 0.799%, respectively. The Lissajous patterns in Figure 9 show the phase relationships between output signals I_{O1} - I_{O2}, I_{O2} - I_{O3}, and I_{O3} - I_{O1}.

In addition, the sinusoidal waveforms of voltage outputs are depicted in Figures 10 and 11, which are transient and steady state, respectively. Figure 12 depicts the THD and spectrum frequencies of the sinusoidal signals, where THD is defined as 0.343 %, 0.324 %, and 0.298 % of V_{O1}, V_{O2}, and V_{O3}, respectively.

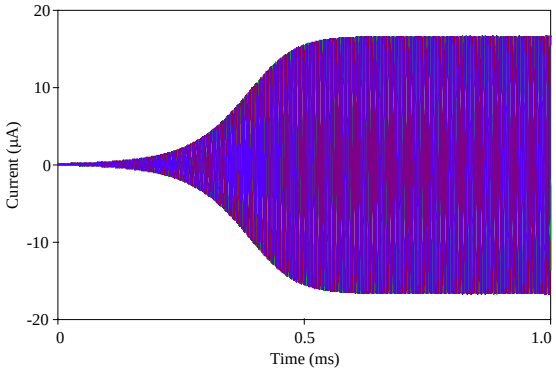

Figure 6. The current waveforms of proposed MSO during transient-state

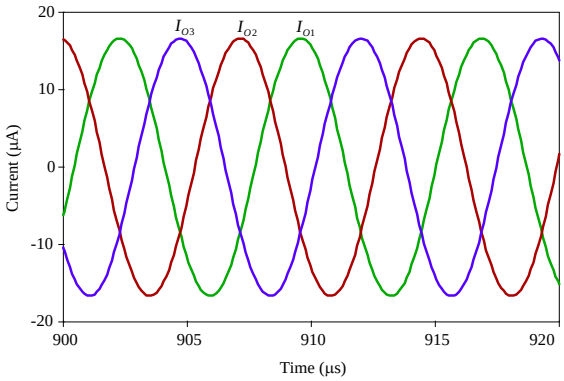

Figure 7. The current waveforms of proposed MSO during steady-state

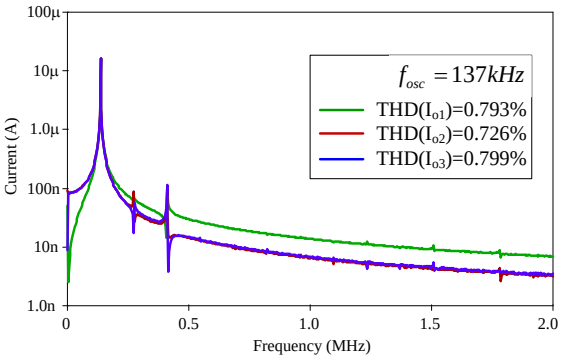

Figure 8. Frequency spectrum of I_{O1}, I_{O2} and I_{O3}

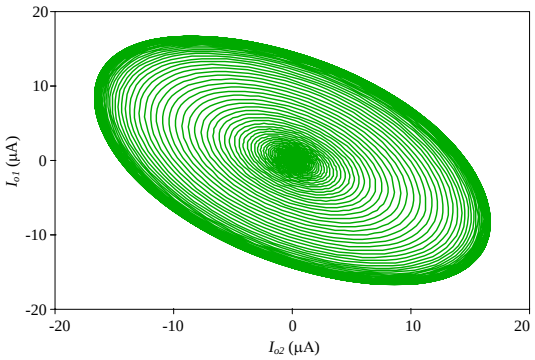

(a)

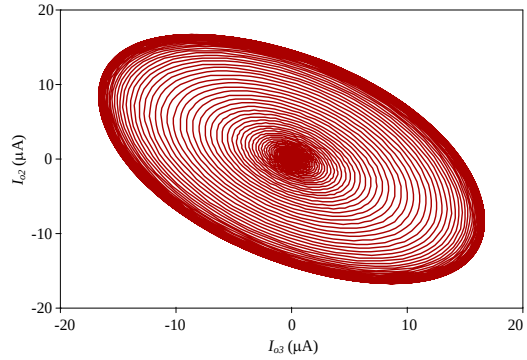

(b)

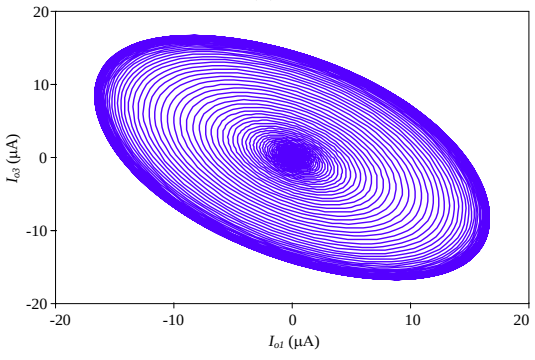

(c)

Figure 9. The Lissajous patterns (a) I_{O1}-I_{O2}, (b) I_{O2}-I_{O3}, and (c) I_{O3} – I_{O1}

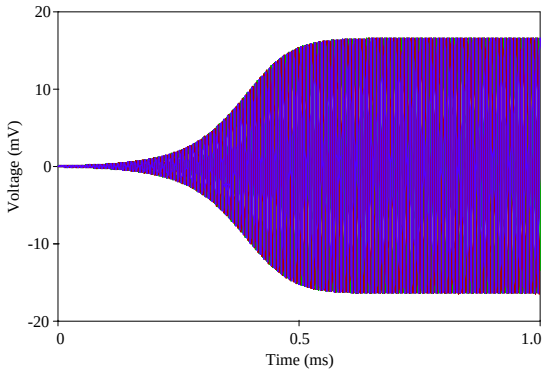

Figure 10. The voltage waveforms of proposed MSO during transient state

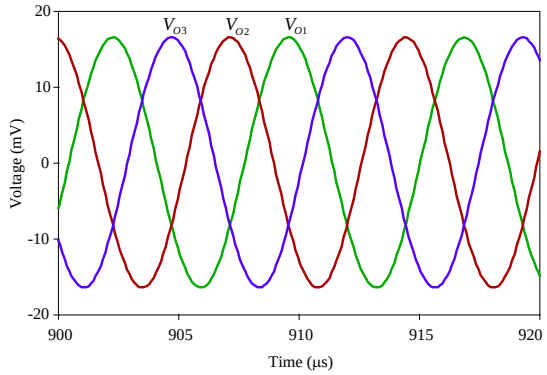

Figure 11. The current waveforms of proposed MSO during steady-state

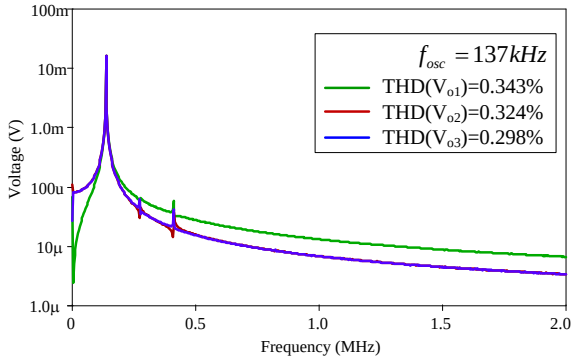

Figure 12. Frequency spectrum of V_{O1}, V_{O2} and V_{O3}

The phase relation of V_{O1} - V_{O2}, V_{O2} - V_{O3}, and V_{O3} - V_{O1} are plotted in Figure 13. As demonstrated in Figure 14, the simulation results and theoretical calculation of the oscillation frequency can be plotted by adjusting the resistor values between 400Ω and 2kΩ while keeping the ratio of resistor-to-DC bias constant. The simulation frequencies range between 137 kHz and 612 kHz, which are close to the theoretical calculation.

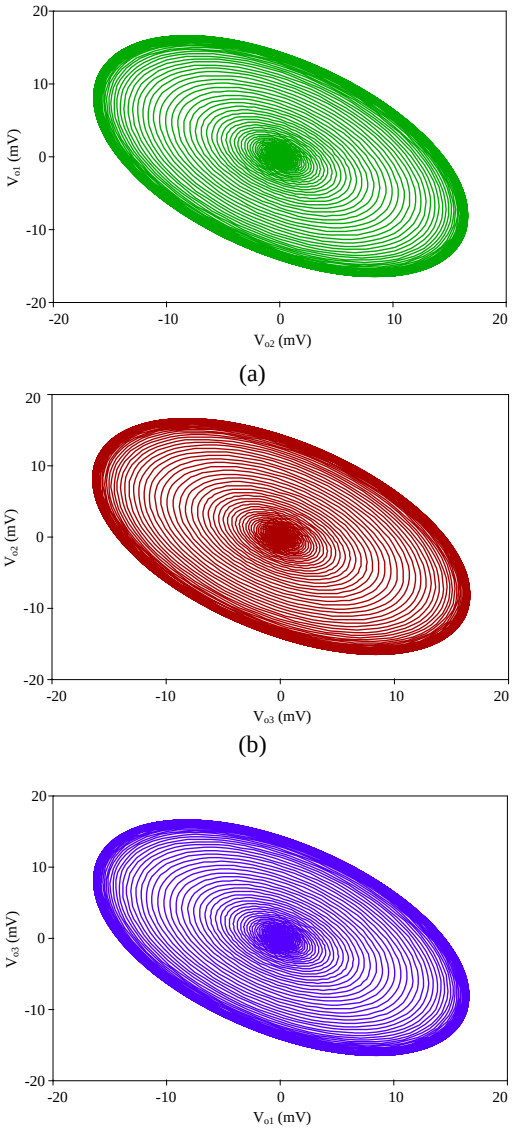

Figure 13. The Lissajous pattern (a) V_{O1}-$V_{O'}$, (b) V_{O2}-$V_{O'}$, and (c) $V_{O'}$- $V_{O'}$

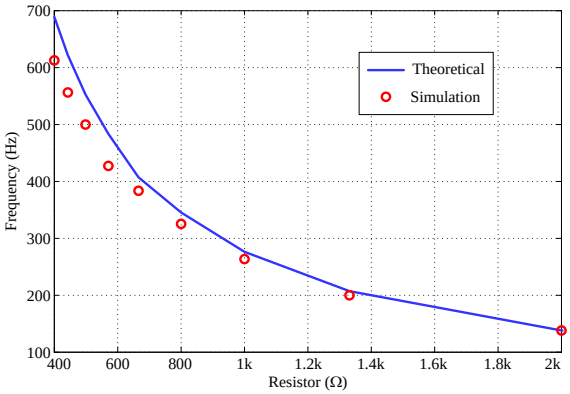

Figure 14. The oscillation frequency adjustment

However, in practice, the tolerance errors of passive conponents affect the performance of proposed MSO circuits. These tolerance errors can be analyzed by using the Monte Carlo Analysis. The Gaussian probability distributions were set with 100 trials, which had a 1% tolerance error for each resistors and a 10% tolerance error for each capacitors. The simulation result can be plotted on the histogram of spread space FO as shown in Figure 15. The minimum and maximum of FO are 121.558 kHz and 157.007 kHz, respectively. The mean and median of FO are 136.054 kHz and ١٣٥.789 kHz, respectively.

To confirm the performance of the proposed MSO so that it conforms to the theory and the simulation, the circuit in Figure 3(c) is chosen as an experimental example for N = 3. The DVCCTA has been constructed using commercial ICs: AD830, AD844, and LM13700N as shown in Figure 16. The setting for the CO was set by a value of g_mR greater than 2 which is set by configuring a value of R = 2 kΩ and bias currents are about I_B = 50 µA. The capacitors are chosen with a value of C = 1 nF. The input bias currents were tested with a Keysight 34461A and using a Siglent SPD3303C power supply was used to power the circuit by ±5 V. The Keysight DSOX3024T oscilloscope is used to display and measure sinusoidal waveforms parameters. The experimental is set up by the hardware used in Figure 17. The experimental results in Figure 18 are show the sinusoidal output waveforms of V_{O1}, V_{O2}, and V_{O3} which can generate a frequency of oscillation at 131.24 kHz. The calculated FO yields 137.83 kHz, while the FO of experimental had a 4.78% error frequency. The phase relationships between V_{O1} - V_{O2}, V_{O2} -V_{O3}, and V_{O3} - V_{O1} are 118.36°, 121.46°, and 120.24°, respectively, which is in accord with the theory proposed. The frequency spectrum of V_{O1}, V_{O2}, and V_{O3} are displayed in Figure 19 and the total harmonic distortions were measured at 0.56%, 0.44%, and 0.78%, respectively. In addition, the experimental results in Figures 19(a), 19(b) and 19(c) show the the magnitude of the first harmonic was higher

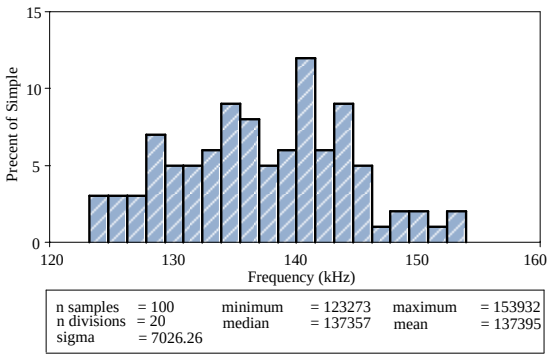

Figure 15. The histograms of the possible spread of FO

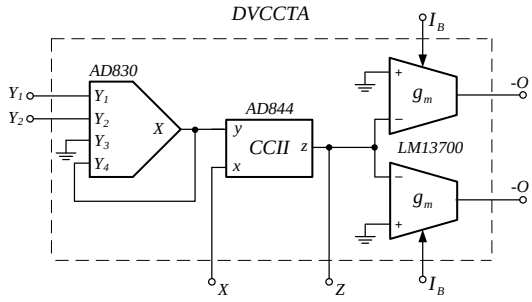

Figure 16. The DVCCTA for experimental test

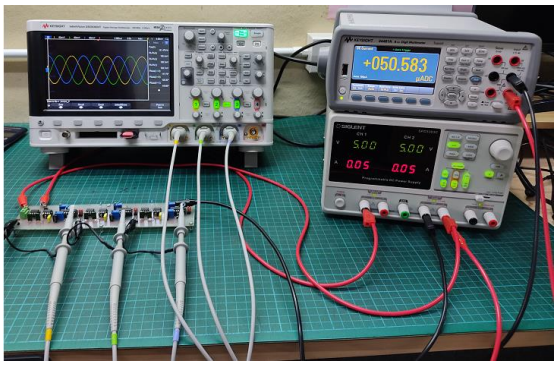

Figure 17. The experimental setup

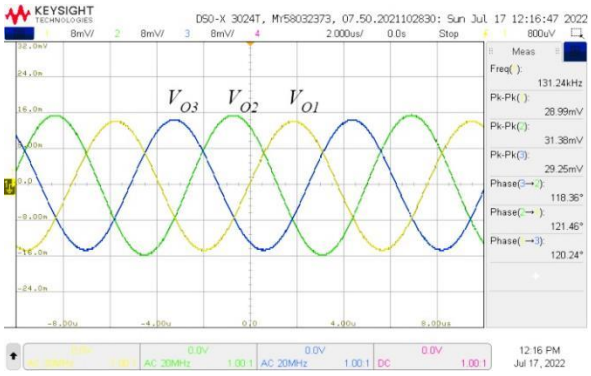

Figure 18. The output waveforms of the MSO

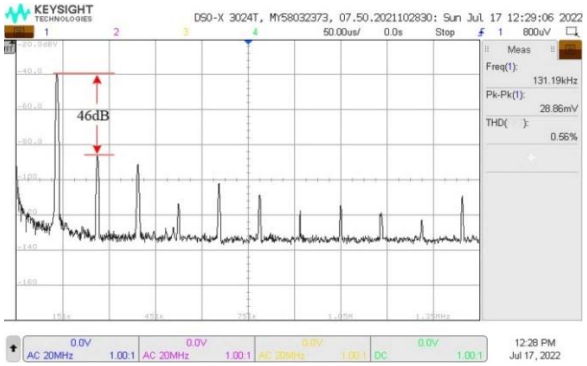

(a)

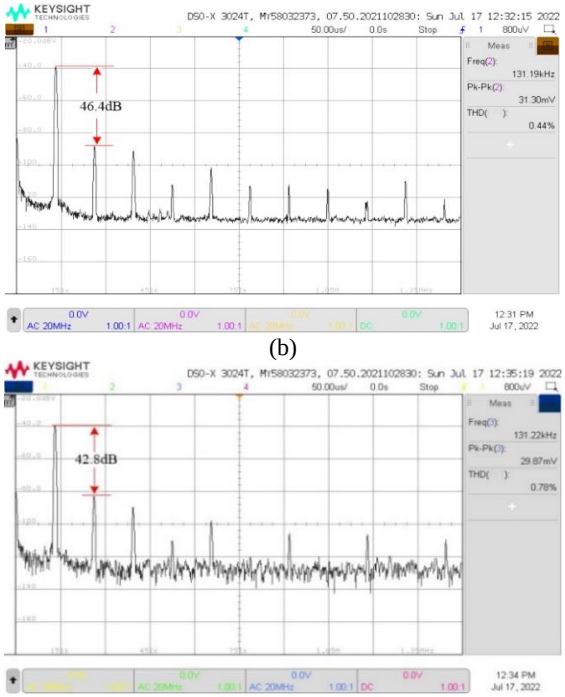

Figure 19. Spectrums frequencies of the MSO (a) V_{O1}, (b) V_{O2}, and (c) V_{O3}

than the second harmonic by about 46 dB, 46.4 dB and 42.8 dB, respectively. It is pleasing that simulation and experiment results correspond well with theoretical analysis.

4. CONCLUSION

The three circuits of mixed-mode MSO using DVCCTA have been presented. They consist of a single DVCCTA, a single grounded resistor, and a single grounded capacitor for each phase. The proposed MSOs are both equally phased and of equal amplitude, which do not require additional amplifier for sinusoidal oscillation. Moreover, high impedance output currents are cascaded to the load without current buffers. Also, the oscillation can be adjusted simultaneously by the oscillation frequency using the electronic method. Finally, to confirm the validity of the proposed MSOs theory, it has been simulated with the PSPICE program and experimentally with commercially available ICs. The simulated and experimental results are completely consistent with the theory.

5. ACKNOWLEDGEMENT

This research was supported by a grant from the Faculty of Engineering, Rajamangala University of Technology, Isan, Khon Kaen Campus, Khon Kaen, Thailand.

6. REFERENCES

1. Dunlop, J., "Telecommunications engineering, Routledge, (2017).
2. Tomasi, W., "Electronic communications system: Fundamentals through advanced, 5/e, Pearson Education India, (2009).
3. Kazmierkowski, M.P. and Silva, F.A., "Power electronics handbook, (rashid, mh; 2011)[book news]", ***IEEE Industrial Electronics Magazine***, Vol. 2, No. 5, (2011), 54-55.
4. Senani, R., Bhaskar, D., Singh, V.K. and Sharma, R., "Sinusoidal oscillators and waveform generators using modern electronic circuit building blocks, Springer, Vol. 622, (2016).
5. Jaikla, W., Talabthong, P., Siripongdee, S., Supavarasuwat, P., Suwanjan, P. and Chaichana, A., "Electronically controlled voltage mode first order multifunction filter using low-voltage low-power bulk-driven otas", ***Microelectronics Journal***, Vol. 91, (2019), 22-35. https://doi.org/10.1016/j.mejo.2019.07.009
6. Thongdit, P., Kunto, T. and Prommee, P., "Ota high pass filter-based multiphase sinusoidal oscillator", in 2015 38th International Conference on Telecommunications and Signal Processing (TSP), IEEE., (2015), 1-5.
7. Prommee, P. and Dejhan, K., "An integrable electronic-controlled quadrature sinusoidal oscillator using cmos operational transconductance amplifier", ***International Journal of Electronics***, Vol. 89, No. 5, (2002), 365-379. doi: 10.1080/713810385.
8. Skotis, G. and Psychalinos, C., "Multiphase sinusoidal oscillators using second generation current conveyors", ***AEU-international Journal of Electronics and Communications***, Vol. 64, No. 12, (2010), 1178-1181. https://doi.org/10.1016/j.aeue.2009.11.013
9. Wu, D.-S., Liu, S.-I., Hwang, Y.-S. and Wu, Y.-P., "Multiphase sinusoidal oscillator using second-generation current conveyors", ***International Journal of Electronics***, Vol. 78, No. 4, (1995), 645-651. doi: 10.1080/00207219508926198.
10. Abuelmaatti, M.T. and Al-Qahtani, M.A., "A new current-controlled multiphase sinusoidal oscillator using translinear current conveyors", ***IEEE Transactions on Circuits and Systems II: Analog and Digital Signal Processing***, Vol. 45, No. 7, (1998), 881-885. doi: 10.1109/82.700937.
11. Loescharataramdee, C., Kiranon, W., Sangpisit, W. and Yadum, W., "Multiphase sinusoidal oscillators using translinear current conveyors and only grounded passive components", in Proceedings of the 33rd Southeastern Symposium on System Theory (Cat. No. 01EX460), IEEE., (2001), 59-63.
12. Tangsrirat, W., Tanjaroen, W. and Pukkalanun, T., "Current-mode multiphase sinusoidal oscillator using cdta-based allpass sections", ***AEU-international Journal of Electronics and Communications***, Vol. 63, No. 7, (2009), 616-622. https://doi.org/10.1016/j.aeue.2008.05.001
13. Jaikla, W., Siripruchyanun, M., Biolek, D. and Biolkova, V., "High-output-impedance current-mode multiphase sinusoidal oscillator employing current differencing transconductance amplifier-based allpass filters", ***International Journal of Electronics***, Vol. 97, No. 7, (2010), 811-826. doi: 10.1080/00207211003733288.
14. Tangsrirat, W. and Tanjaroen, W., "Current-mode multiphase sinusoidal oscillator using current differencing transconductance amplifiers", ***Circuits, Systems & Signal Processing***, Vol. 27, (2008), 81-93. doi: 10.1007/s00034-007-9010-y.
15. Klahan, K., Tangsrirat, W. and Surakampontorn, W., "Realization of multiphase sinusoidal oscillator using cdbas", in The 2004 IEEE Asia-Pacific Conference on Circuits and Systems, 2004. Proceedings., IEEE. Vol. 2, (2004), 725-728.
16. Sagbas, M., Ayten, U.E., Herencsar, N. and Minaei, S., "Voltage-mode multiphase sinusoidal oscillators using cbtas", in 2012 35th

International Conference on Telecommunications and Signal Processing (TSP), IEEE., (2012), 421-425.

17. Pandey, R., Pandey, N., Mullick, R., Yadav, S. and Anurag, R., "All pass network based mso using otra", ***Advances in Electronics***, Vol. 2015, (2015). https://doi.org/10.1155/2015/382360
18. Pandey, R. and Bothra, M., "Multiphase sinusoidal oscillators using operational trans-resistance amplifier", in 2009 IEEE Symposium on Industrial Electronics & Applications, IEEE. Vol. 1, (2009), 371-376.
19. Jaikla, W. and Prommee, P., "Electronically tunable current-mode multiphase sinusoidal oscillator employing cccdta-based allpass filters with only grounded passive elements", ***Radioengineering***, Vol. 20, No. 3, (2011), 594-599.
20. Kumngern, M., "Current-mode multiphase sinusoidal oscillator using current-controlled current differencing transconductance amplifiers", in 2010 IEEE Asia Pacific Conference on Circuits and Systems, IEEE., (2010), 728-731.
21. Kumngern, M., "Current-controlled current-mode multiphase oscillator using cccdtas", in 2011 IEEE Symposium on Computers & Informatics, IEEE., (2011), 188-191.
22. Uttaphut, P., Mekhum, W. and Jaikla, W., "Current-mode multiphase sinusoidal oscillator using cccctas and grounded elements", in 2011 IEEE 9th International New Circuits and systems conference, IEEE., (2011), 345-349.
23. Gupta, P. and Pandey, R., "Dual output voltage differencing buffered amplifier based active-c multiphase sinusoidal oscillator", ***International Journal of Engineering, Transactions C: Aspects***, Vol. 34, No. 6, (2021), 1438-1444.
24. Pitaksuttayaprot, K., Phanrattanachai, K. and Jaikla, W., "Electronically adjustable multiphase sinusoidal oscillator with high-output impedance at output current nodes using vdccs", ***Electronics***, Vol. 11, No. 19, (2022), 3227. doi: 10.3390/electronics11193227.
25. Jaikla, W., Khateb, F., Kulej, T. and Pitaksuttayaprot, K., "Universal filter based on compact cmos structure of vddda", ***Sensors***, Vol. 21, No. 5, (2021), 1683. doi: 10.3390/s21051683.
26. Jaikla, W., Khateb, F., Kumngern, M., Kulej, T., Ranjan, R.K. and Suwanjan, P., "0.5 v fully differential universal filter based on multiple input otas", ***IEEE Access***, Vol. 8, (2020), 187832-187839. doi: 10.1109/ACCESS.2020.3030239.
27. Jantakun, A., Pisutthipong, N. and Siripruchyanun, M., "A synthesis of temperature insensitive/electronically controllable floating simulators based on dv-cctas", in 2009 6th International Conference on Electrical Engineering/Electronics, Computer, Telecommunications and Information Technology, IEEE. Vol. 1, (2009), 560-563.
28. Bhushan, M. and Newcomb, R., "Grounding of capacitors in integrated circuits", ***Electronics Letters***, Vol. 3, No. 4, (1967), 148-149.
29. Chauhan, D.S., Tomar, R. and Singh, S., "A new trans-admittance-mode biquad filter suitable for low voltage operation", ***International Journal of Engineering, Transactions B: Applications,*** Vol. 28, No. 12, (2015), 1738-1745. doi: 10.5829/idosi.ije.2015.28.12c.06.
30. Keramatzadeh, A. and Farshidi, E., "A new approach for low voltage cmos based on current-controlled conveyors", ***International Journal of Engineering, Transactions B: Applications***, Vol. 27, No. 5, (2014), 723-730. doi: 10.5829/idosi.ije.2014.27.05b.07.
31. Frey, D., "Log-domain filtering: An approach to current-mode filtering", ***IEE Proceedings G (Circuits, Devices and Systems)***, Vol. 140, No. 6, (1993), 406-416.
32. Bajer, J., Lahiri, A. and Biolek, D., "Current-mode ccii+ based oscillator circuits using a conventional and a modified wien-bridge with all capacitors grounded", ***Radioengineering***, Vol. 20, No. 1, (2011), 245-250. https://www.radioeng.cz/fulltexts/2011/11_01_245_251.pdf

Persian Abstract

چکیده

این مقاله در مورد نوسان سازهای سینوسی چند فازی است که از تقویت کننده ترانس رسانایی انتقال جریان ولتاژ دیفرانسیل (DVCCTA) ساخته شده اند و از تمام اجزای غیرفعال زمین شده استفاده می کنند. اسیلاتورهای سینوسی چند فازی پیشنهادی یک DVCCTA، یک مقاومت زمینی تک و یک خازن برای هر فاز ارائه می‌کنند که برای اجرای مدار مجتمع مناسب است. علاوه بر این، خروجی های سینوسی به طور همزمان جریان و ولتاژ تولید می کنند. سیگنال های جریان خروجی دارای امپدانس های بالایی هستند که اتصال مستقیم آنها را به مدار یا مرحله بعدی آسان تر می کند. مدارهای پیشنهادی می‌توانند سیگنال‌های سینوسی چند فازی تولید کنند که هم فاز و هم در دامنه هستند. نوسان را می توان به طور همزمان فرکانس نوسان را با روش الکترونیکی تنظیم کرد. شبیه‌سازی با برنامه PSPICE و آزمایشی با آی‌سی‌های تجاری موجود (AD830، AD844 و LM13700N) نشان داد. نتایج نشان می دهد که کارایی مدار کاملاً با تئوری مطابقت دارد.